

Structure and Function of YghU, a Nu-Class Glutathione Transferase Related to YfcG from *Escherichia coli*^{†,‡}

Nina V. Stourman,^{§,⊥} Megan C. Branch,[§] Matthew R. Schaab,[§] Joel M. Harp,[§] Jane E. Ladner,^{||} and Richard N. Armstrong^{*,§}

[§]Departments of Biochemistry and Chemistry, Center in Molecular Toxicology, and Vanderbilt Institute of Chemical Biology, Vanderbilt University, Nashville, Tennessee 37232-0146, United States, and ^{||}Institute for Bioscience and Biotechnology Research, University of Maryland, Gudelsky Drive, Rockville, Maryland 20850, United States. [⊥]Current address, Department of Chemistry, Youngstown State University, Youngstown, OH 44555.

Received November 22, 2010; Revised Manuscript Received January 10, 2011

ABSTRACT: The crystal structure (1.50 Å resolution) and biochemical properties of the GSH transferase homologue, YghU, from *Escherichia coli* reveal that the protein is unusual in that it binds two molecules of GSH in each active site. The crystallographic observation is consistent with biphasic equilibrium binding data that indicate one tight ($K_{d1} = 0.07 \pm 0.03$ mM) and one weak ($K_{d2} = 1.3 \pm 0.2$ mM) binding site for GSH. YghU exhibits little or no GSH transferase activity with most typical electrophilic substrates but does possess a modest catalytic activity toward several organic hydroperoxides. Most notably, the enzyme also exhibits disulfide-bond reductase activity toward 2-hydroxyethyl disulfide [$k_{\text{cat}} = 74 \pm 6$ s⁻¹, and $k_{\text{cat}}/K_M^{\text{GSH}} = (6.6 \pm 1.3) \times 10^4$ M⁻¹ s⁻¹] that is comparable to that previously determined for YfcG. A superposition of the structures of the YghU·2GSH and YfcG·GSSG complexes reveals a remarkable structural similarity of the active sites and the 2GSH and GSSG molecules in each. We conclude that the two structures represent reduced and oxidized forms of GSH-dependent disulfide-bond oxidoreductases that are distantly related to glutaredoxin 2. The structures and properties of YghU and YfcG indicate that they are members of the same, but previously unidentified, subfamily of GSH transferase homologues, which we suggest be called the nu-class GSH transferases.

The chromosome of *Escherichia coli* K-12 harbors nine genes encoding members of the glutathione (GSH)¹ transferase superfamily (1). The functions of most of these proteins have not been experimentally established. The GSH transferases typically catalyze the addition of the tripeptide to endogenous or xenobiotic molecules bearing electrophilic functional groups (Scheme 1). There are several examples, however, in which members of this protein superfamily have other very distinct functions such as redox chemistry, ion transport, and the regulation of transcription or translation (1–8). It is likely that several of the GSH transferase homologues in *E. coli* have functions other than the catalytic one illustrated in Scheme 1. In this regard, we recently reported that YfcG, which has poor GSH transferase activity toward typical electrophilic substrates, has an excellent disulfide-bond oxidoreductase activity as shown in Scheme 2 (9).

To make matters more interesting, there are two predominant redox-active thiols in *E. coli*, GSH and glutathionylspermidine

(GspSH) (10). Glutathione is the principal thiol in the bacterium under aerobic conditions, while GspSH predominates during anaerobic conditions (9–11). The thiol tone is controlled by glutathionylspermidine synthetase/amidase (GSS), a bifunctional enzyme that catalyzes the ATP-dependent condensation of the glycyl carboxylate of GSH with the N1 atom of spermidine in the forward direction and the hydrolysis of the resulting amide in the reverse direction (12, 13). How this enzyme is regulated has not been elucidated. It could be that one of the GSH transferase homologues in *E. coli* is a regulatory protein for GSS or that one or more of the homologues is a GspSH transferase.

Several years ago we noted that the *gss* gene in *E. coli* was located next to the *yghU* (b2989) gene that encodes one of the GSH transferase homologues (1). On the basis of this observation, we suggested that the YghU protein might be involved in the regulation of the synthesis or the degradation of GspSH, or that YghU is a GspSH transferase. In this report, we describe the structural and biochemical characterization of YghU that points to a different function for this protein, that of a disulfide-bond oxidoreductase closely related to YfcG and more distantly related to glutaredoxin 2 from *E. coli*.

EXPERIMENTAL PROCEDURES²

Materials. *E. coli* K-12 genomic DNA was from ATCC (Manassas, VA). Primers were custom ordered from Invitrogen

[†]Supported by Grants R01 GM030910, P30 ES000267, T32 ES007028, and T32 GM065086 from the National Institutes of Health.

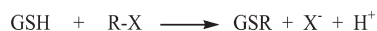
[‡]The atomic coordinates and structure factors for YghU have been deposited in the Protein Data Bank as entry 3C8E.

*To whom correspondence should be addressed. Phone: (615) 343-2920. Fax: (615) 343-2921. E-mail: r.armstrong@vanderbilt.edu.

Abbreviations: GSH, glutathione; GSSG, glutathione disulfide; GspSH, glutathionylspermidine; HEPES, *N*-(2-hydroxyethyl)piperazine-*N'*-ethanesulfonic acid; IPTG, isopropyl β-thiogalactopyranoside; PCR, polymerase chain reaction; DEAE, diethylaminoethyl; DTT, dithiothreitol; EDTA, ethylenediaminetetraacetic acid; LB, Luria broth; PEG, polyethylene glycol; SP, sulfopropyl; PEG, polyethylene glycol; CDNB, 1-chloro-2,4-dinitrobenzene; NADPH, nicotinamide adenine dinucleotide phosphate; Bis-Tris, 2,2-bis(hydroxymethyl)-2,2',2''-nitrioltriethanol; MES, 2-(*N*-morpholino)ethanesulfonic acid; BSA, albumin, bovine fraction V.

²Certain commercial materials, instruments, and equipment are identified in this paper to specify the experimental procedure as completely as possible. In no case does such identification imply a recommendation or endorsement by the National Institute of Standards and Technology, nor does it imply that the materials, instruments, or equipment identified is necessarily the best available for the purpose.

Scheme 1



Scheme 2



(Carlsbad, CA). Restriction enzymes were from New England Biolabs (Ipswich, MA). The pET20b(+) vector and B834(DE3) cells were from EMB Chemicals, Inc. (Gibbstown, NJ). BL21-Gold(DE3) cells were from Stratagene (La Jolla, CA). Luria broth, ampicillin, NADPH, IPTG, HEPES, DTT, streptomycin sulfate, and MES were all from Research Products International (Mt. Prospect, IL). EDTA, ammonium acetate, glutathione, glutathione disulfide, CDNB, ethacrynic acid, *trans*-4-phenyl-3-buten-2-one, 1,2-epoxy-3-(4-nitrophenoxy)propane, 1,4-dichloro-2-nitrobenzene, *tert*-butyl hydroperoxide, cumene hydroperoxide, *Saccharomyces cerevisiae* glutathione reductase, and all amino acids were ordered from Sigma Aldrich (St. Louis, MO). DEAE-Cellulose and SP-Sepharose resins were obtained from GE Healthcare (Piscataway, NJ). Hydrogen peroxide and linoleic acid was from Fisher Scientific (Pittsburgh, PA). The soybean lipoxidase was from VWR (West Chester, PA). The 15(S)-HpETE substrate was a generous gift from A. Brash (Vanderbilt University).

Cloning, Expression, and Purification of YghU. The *yghU* gene was amplified from the *E. coli* K-12 genomic DNA (ATCC) using primers containing restriction sites for *Nde*I and *Eco*RI. The forward primer was AAA AAA TCT AGA CAT ATG ACA GAC AAT ACT TAT CAG CCC and the reverse primer TTT GGA TCC G AA TTC TTA CCC CTG ACG CTT ATC TTC CG.

The *yghU* gene was digested and ligated into the *pET20b* vector. *E. coli* BL21(DE3) cells were transformed with the *pET20b(yghU)* plasmid; a liquid culture of the transformed bacteria was grown overnight from a single colony in LB medium containing 100 $\mu\text{g/mL}$ ampicillin at 37 °C. The cells were diluted 100-fold in fresh medium and grown to an OD_{600} of ~ 0.8 . Protein production was induced by addition of 0.4 mM IPTG. The cells were grown for 4 h at 30 °C to prevent the formation of inclusion bodies. The cells were harvested by centrifugation at 6000g for 10 min, and the pellet was frozen at -20 °C for storage. The frozen pellet was resuspended in 20 mM HEPES and 1 mM EDTA (pH 7.0), lysed by sonication, and centrifuged at 17000g for 30 min. Supernatant was treated with streptomycin sulfate (10 mg/mL), centrifuged for 30 min at 17000g, and dialyzed overnight against 20 mM HEPES and 1 mM EDTA (pH 7.5). The solution was loaded on a DEAE-cellulose column equilibrated with 20 mM HEPES and 1 mM EDTA (pH 7.5) and eluted from the column with a linear gradient of NaCl (from 0 to 0.4 M) in the same buffer. Fractions containing the protein (determined by A_{280} and sodium dodecyl sulfate–polyacrylamide gel electrophoresis) were pooled together, dialyzed against 20 mM MES and 1 mM EDTA (pH 5.8), loaded on an SP-Sepharose column equilibrated with 20 mM MES and 1 mM EDTA (pH 5.8), and eluted with the linear gradient of NaCl (from 0 to 0.4 M) in the same buffer. Fractions containing the protein (determined by A_{280} and sodium dodecyl sulfate–polyacrylamide gel electrophoresis) were pooled together, dialyzed against 20 mM KH_2PO_4 and 1 mM EDTA (pH 7.0), concentrated, and flash-frozen.

The selenomethionine derivative was prepared from *E. coli* B834 DE3 cells transformed with the expression vector containing

the *yghU* insert. A single colony was used to inoculate a 100 mL culture of M9 medium containing 100 $\mu\text{g/mL}$ ampicillin. The culture was grown overnight at 37 °C. A 10 mL aliquot of the overnight culture was used to inoculate a 1 L culture of M9 medium supplemented with 30 mg of all common amino acids. The cultures were grown at 37 °C with shaking at 250 rpm. When the OD_{600} reached 0.6, the cells were harvested by centrifugation at 8000g for 10 min. The cells were resuspended in 1 L of M9 medium supplemented with 30 mg of every common amino acid and 50 mg of selenomethionine substituted for methionine. The cells were induced by the addition of 100 mg of IPTG. The cells were grown at 15 °C and 225 rpm for 16 h. The cells were harvested by centrifugation at 8000g for 10 min. The cell paste was frozen and stored at -80 °C. The selenomethionyl enzyme was purified as described previously for the native protein.

Steady-State Enzyme Kinetics. The GSH transferase activity of YghU was assayed with several common substrates, including CDNB, ethacrynic acid, *trans*-4-phenyl-3-buten-2-one, 1,2-epoxy-3-(4-nitrophenoxy)propane, and 1,4-dichloro-2-nitrobenzene. With these potential substrates, YghU exhibited measurable activity with only CDNB. Reactions with CDNB were followed with a Perkin-Elmer Lambda 45 spectrophotometer at 25 °C in 1 mL cuvettes. For each reaction, 0.7 μM YghU was preincubated with various concentrations of GSH (from 0.5 μM to 20 mM) or GspSH (from 8 μM to 1 mM) in 100 mM KH_2PO_4 buffer (pH 7.0) for 4 min. The reaction was initiated via addition of a solution of CDNB in CH_3CN to a final concentration of 2 mM. The rate of production of the GSH or GspSH conjugate with CDNB was calculated using a linear regression to fit the initial rate measured by the increase in absorbance at 340 nm ($\Delta\epsilon = 9600 \text{ M}^{-1} \text{ cm}^{-1}$). When necessary, corrections were made for the uncatalyzed reaction between the thiols and CDNB. All measurements were taken in triplicate and averaged. Data were analyzed with a nonlinear least-squares fit to the Michaelis–Menten equation.

The assays for estimating the inhibition of the addition of GSH to CDNB by GSSG were conducted at 25 °C in 100 mM KH_2PO_4 (pH 6.5) containing 3.0 μM YghU and 250 μM CDNB. The GSH concentration was varied between 30 and 400 μM . The inhibited reaction mixture contained 15 μM GSSG.

The disulfide-bond reductase activity of YghU was measured with the model substrate, 2-hydroxyethyl disulfide, at pH 8.0 and 25 °C by the coupled assay previously described (9, 14). The peroxidase activity of YghU was evaluated with several peroxides, including hydrogen peroxide, *tert*-butyl hydroperoxide, cumene hydroperoxide, linoleic acid 13(S)-hydroperoxide, and 15(S)-HpETE. Little or no activity was detected with hydrogen peroxide and *tert*-butyl hydroperoxide. The linoleic acid hydroperoxide was synthesized using a method similar to that described in ref 15. Briefly, 1 mM linoleic acid was combined with 0.1 mg/mL soybean lipoyxygenase in 100 mM Tris-HCl buffer (pH 7.4). The product was extracted with chloroform, dried under argon, and resuspended in methanol. The concentration of linoleic acid 13(S)-hydroperoxide was measured by A_{234} using an ϵ_{234} of $25000 \text{ M}^{-1} \text{ cm}^{-1}$. The organic hydroperoxidase activity of YghU with cumene hydroperoxide and linoleic acid hydroperoxide was measured with the coupled assay with GSH reductase from yeast according to the method described in ref 16. Reactions were followed with a Perkin-Elmer Lambda 45 spectrophotometer at 25 °C in 1 mL cuvettes. Reaction mixtures contained 1 μM YghU, and GSH at concentrations between 0.10 and 4.0 mM and 0.8 unit of GSH reductase from yeast in 100 mM KH_2PO_4

(pH 7.0) were preincubated at 25 °C for 5 min, followed by addition of NADPH to a final concentration of 0.15 mM and incubation for 3 min. The reactions were initiated by addition of cumene hydroperoxide to a final concentration 1 mM or linoleic acid 13(*S*)-hydroperoxide to a final concentration of 50 μ M. The decrease of absorbance at 340 nm ($\Delta\epsilon = -6220 \text{ M}^{-1} \text{ cm}^{-1}$) was monitored over 3–5 min and used to calculate the initial rate. An HPLC-based method similar to that described in ref 17 was used to determine the lipid peroxidase activity of YghU with 15(*S*)-HpETE. Reaction mixtures containing 0.15 μ M protein, 3 mM GSH, and various concentrations of 15(*S*)-HpETE were incubated in 50 μ L of 100 mM KH_2PO_4 buffer (pH 7.0) containing 0.005% BSA (w/v). After 3 min, the reaction was terminated with 100 μ L of acetonitrile containing 0.2% acetic acid. Before analysis, 50 μ L of water was added and the protein was removed by centrifugation (10 min at 14000 rpm). Samples were analyzed using reverse-phase HPLC with a Beckman Ultrasphere C18 column (4.6 mm \times 25 cm). The mobile phase was an acetonitrile/ H_2O /acetic acid mixture (60:40:0.01, v/v) with a flow rate of 1.0 mL/min. A photodiode array detector (Waters) tuned to 236 nm was used to measure absorbance values, and Empower (Waters Corp.) was used to determine peak areas. Amounts of 15(*S*)-HETE were calculated on the basis of the peak area from known amounts of standard 15(*S*)-HETE (retention time of 10.9 min) and 15(*S*)-HpETE (retention time of 11.9 min). All measurements of peroxidase activity were taken in triplicate and averaged. Data were fit to the Michaelis–Menten equation by nonlinear regression analysis.

Steady-State Fluorescence Titrations. Dissociation constants for the complex of YghU with GSH and GspSH were determined by titration of the intrinsic fluorescence of the protein. Fluorescence measurements were conducted at 25 °C on a SPEX Fluorolog-3 spectrofluorimeter (Jobin Yvon Horiba, Edison, NJ) in the constant-wavelength mode. The samples were excited at 295 nm, and the emission was collected at 340 nm and integrated over a period over 30 s. All measurements were taken in triplicate and averaged. Inner filter effects were taken into consideration using eq 1 to calculate a corrected fluorescence, F_c (18).

$$F_c = F \times \text{antilog}[(A_{295} + A_{340})/2] \quad (1)$$

The change in fluorescence intensity of 1 μ M protein in 20 mM KH_2PO_4 buffer (pH 7.0) was measured after a 5 min preincubation with GSH to a final concentration of 0.025–10 mM or GspSH to a final concentration of 0.025–8 mM. The corrected titration data were fit by nonlinear regression analysis with GraphPad starting with initial estimates for values of K_d and ΔF derived from the primary data. The titration data for GSH were fit to a two-site binding model with eq 2, while the binding data for GspSH were fit to a single-site binding model (eq 3).

$$F = ([S]\Delta F_1)/([S] + K_{d1}) + ([S]\Delta F_2)/([S] + K_{d2}) \quad (2)$$

$$F = ([S]\Delta F)/([S] + K_d) \quad (3)$$

Cytoscape Cluster Analysis of the GSH Transferase Superfamily. The data used to construct the network in Figure 6 were compiled and filtered by S. Brown at The California Institute for Quantitative Biomedical Research at the University of California, San Francisco (P. Babbitt, Principle Investigator). It can be downloaded from <http://babbittlab.compbio.ucsf.edu/glue.html>. The cytoscape software for visualization of these networks is available as a free download from the Cytoscape Consortium

Table 1: Data Collection and Refinement Statistics for the Determination of the Structure of YghU^a

Data Collection	
PDB entry	3C8E
space group	$P2_12_12_1$
cell parameters a, b, c (Å)	58.197, 73.455, 130.810
wavelength of data collection (Å)	1.000
no. of unique reflections	95609
resolution of data (Å)	50–1.41
highest-resolution shell (Å)	1.46–1.41
R_{merge}	0.109 (0.551)
completeness (%)	87.7 (56.5)
redundancy	8.9 (3.0)
Refinement	
resolution limits (Å)	20.0–1.50 (1.58–1.50)
completeness (%)	100 (100)
no. of reflections used	80150 (8027)
no. of reflections for R_{free}	8037 (882)
R_{work}	0.162 (0.215)
R_{free}	0.197 (0.272)
root-mean-square deviation for bond lengths (Å)	0.019
root-mean-square deviation for bond angles (deg)	1.834
average B (Å ²) (protein/water/GSH)	13.8/22.9/12.0

^aValues for the outer resolution shell are given in parentheses.

(<http://www.cytoscape.org>). All full-length sequences in the Pfam GST_N and GST_C families (as of July 2010) were downloaded. Sequences with fewer than 150 amino acids were considered fragments and removed from the data set. The sequence set was filtered to remove sequences that were >60% identical. An all-by-all BLAST of the remaining sequences was then performed with an E value cutoff of 10^{-14} . The resulting networks were visualized in Cytoscape version 2.7.0 using the organic layout. Nodes represent sequences, and edges represent BLAST E values of 10^{-18} or more significance.

Crystallization of YghU. YghU was crystallized by hanging-drop vapor diffusion at 25 °C with a reservoir solution of 0.1 M Bis-Tris and 0.2 M NaCl (pH 5.5) containing 25% (w/v) PEG 3350. The drop consisted of a 1:1 mixture of reservoir solution and a solution of YghU (20 mg/mL) in 30 mM NaH_2PO_4 (pH 7.0) containing 1 mM DTT and 20 mM GSH. Crystals grew in 1 week as long rods. The crystals were transferred to mother liquor supplemented with 35% ethylene glycol as a cryoprotectant before being flash-frozen.

Collection and Processing of Diffraction Data. Crystals were flash-cooled and maintained at 100 K for cryogenic data collection. The quality of the X-ray diffraction by the crystals was screened in-house using a Bruker Microstar microfocus rotating anode X-ray generator with Montel confocal multilayer X-ray optics. In-house data were collected using a Bruker-Nonius X8 kappa goniometer and Proteum PT135 CCD area detector. Crystals were maintained at 100 K using Bruker KryoFlex cryostats.

A native data set was collected using the mail-in crystallography service at beamline 22-BM of the Southeastern Regional Collaborative Access Team (SER-CAT) at the Advanced Photon Source, Argonne National Laboratory (see <http://www.ser.aps.anl.gov/>). A single selenomethionyl derivative crystal was used to collect MAD data at three wavelengths at SER-CAT beamline 22-BM. The crystal was maintained at 100 K. All data were reduced using HKL2000 (19). Data quality statistics for the reflections collected are listed in Table 1.

Data sets for MAD phasing were collected at 0.9793 Å (peak), 0.9792 Å (inflection), and 0.9717 Å (remote) from a single selenomethionyl derivative crystal. The data sets were closely comparable with respect to their quality and completeness. The average statistics for the three data sets were as follows: resolution range = 50–1.89 Å, completeness = 97.7%, redundancy = 6.9, $I/\sigma I$ = 19.3, and linear R factor = 0.087.

Phasing and Structure Refinement. Phasing of the data was accomplished using SHELXC, SHELXD, and SHELXE (20, 21) using the graphical user interface HKL2MAP (22). All four data sets were input into HKL2MAP with the resolution limit set to 2.5 Å. SHELXD found all eight selenium positions with a maximal correlation coefficient of 67.8%. Refinement of positions in SHELXE resulted in a reported contrast of 0.425 and connectivity of 0.905 and pseudo-free correlation coefficient of 74.0%. Visualization of the map clearly showed density for tyrosine side chains with holes in the ring density.

Phases from SHELXE were imported into the CCP4 suite, and a preliminary structure was built using ARP/wARP (23). ARP/wARP was able to build the model to 93% completion. The model from ARP/wARP was then refined using the native data to 1.50 Å combined with rounds of manual inspection and fitting using Xfit (24).

The final model was refined with REFMAC (25) and consisted of 4649 non-hydrogen protein atoms, four GSH molecules (80 atoms), and 471 solvent atoms. The A chain is missing residues 1–4, and the electron density for residue 5 is poor. Chain B is missing residues 1–5, and residues 15–18 have very poor electron density. Alternative conformations are included for 11 residues in chain A and 12 residues in chain B. Refinement statistics are listed in Table 1.

RESULTS

Initial Characterization of YghU. The *yghU* gene was amplified from genomic DNA, overexpressed in *E. coli*, and purified as described above. The protein behaved as a dimer on gel-filtration chromatography (data not shown). The YghU protein has a modest GSH transferase activity with 1 mM CDNB ($k_{\text{cat}} = 0.109 \pm 0.005 \text{ s}^{-1}$; $k_{\text{cat}}/K_{\text{M}}^{\text{GSH}} = 1400 \pm 300 \text{ M}^{-1} \text{ s}^{-1}$; $K_{\text{M}}^{\text{GSH}} = 80 \pm 20 \mu\text{M}$). It has no detectable activity toward CDNB with GspSH as the nucleophilic substrate. The protein also exhibited no detectable GSH transferase activity toward several other typical electrophilic substrates, including ethacrynic acid, *trans*-4-phenyl-3-buten-2-one, and 1,2-epoxy-3-(4-nitrophenoxy)propane.

Titration of the intrinsic fluorescence of YghU with GSH reveals a biphasic binding curve with an initial increase in fluorescence ($K_{\text{d1}} = 0.07 \pm 0.03 \text{ mM}$) followed by a decrease in fluorescence ($K_{\text{d2}} = 1.3 \pm 0.2 \text{ mM}$) indicating two binding sites for GSH, one with higher binding affinity than the other as illustrated in Figure 1. This behavior is consistent with either a negative cooperativity in the binding of two molecules of GSH to the dimer or the binding of two molecules of GSH, with different affinities, to each active site in the dimer. A similar titration with GspSH revealed a monophasic binding isotherm with a $K_{\text{d}}^{\text{GspSH}}$ of $1.0 \pm 0.1 \text{ mM}$, a ΔF of $(-3.4 \pm 0.1) \times 10^5$, and an r of 0.990.

Attempts to titrate the intrinsic protein fluorescence with GSSG did not produce sufficient signal (ΔF) for a reliable titration. However, inhibition of the CDNB assay by addition of GSSG suggested $K_{\text{i}} \ll 10 \mu\text{M}$, inasmuch as the observed values of k_{cat} and $k_{\text{cat}}/K_{\text{M}}^{\text{GSH}}$ were decreased 10-fold with the addition of $15 \mu\text{M}$ GSSG. The intrinsically low catalytic activity of YghU

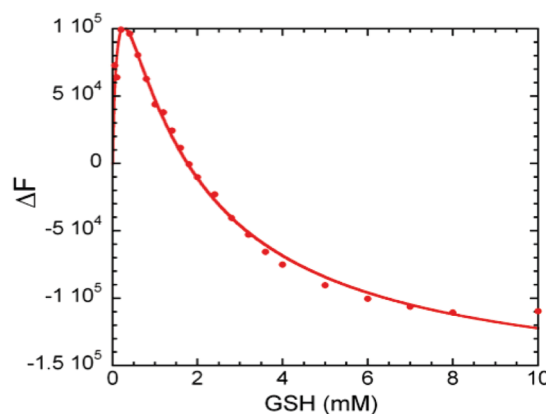


FIGURE 1: Titration of the intrinsic protein fluorescence of YghU with GSH. The experimental data were fit to a two-binding site model (eq 2) with the following values: $K_{\text{d1}} = 0.07 \pm 0.03 \text{ mM}$, and $\Delta F_1 = (2.1 \pm 0.6) \times 10^5$; $K_{\text{d2}} = 1.3 \pm 0.2 \text{ mM}$, and $\Delta F_2 = (-8.7 \pm 0.5) \times 10^5$ ($r = 0.999$).

toward CDNB, the high level of background reaction of GSH with CDNB, and the tight binding of GSSG precluded a reliable determination of the exact mechanism of inhibition and the value of K_{i} . Nevertheless, the indication is that GSSG actually binds more avidly to YghU than GSH.

Does YghU Interact with or Regulate GSS? Our original hypothesis, based on the proximity of the *gss* and *yghU* genes in *E. coli*, was that YghU might regulate GSS activity or be a GspSH transferase (1). The inclusion of YghU in assays of GSS for the synthesis or hydrolysis of GspSH under a variety of conditions provided no clues about a possible role for the protein in the regulation of GSS activity (data not shown). Moreover, the gene knockout of YghU had no significant effect on GspSH levels under anaerobic conditions in *E. coli* (12). In spite of the fact that YghU does bind GspSH with a modest affinity, there is no evidence at this point of its role in utilization, synthesis, or degradation of GspSH.

Structure of YghU. The YghU protein crystallized in the presence of GSH in space group $P2_12_12_1$, and the structure was determined by MAD phasing at a resolution of 1.50 Å. Details of the data collection, structure determination, and refinement can be found in Experimental Procedures. The core of the structure is a classic GSH transferase fold (Figure 2) that is most similar to that of YfcG from *E. coli* (9). The polypeptide of YghU is ~30 residues longer than a typical GSH transferase. This extra length is manifest in a long N-terminal extension that wraps over the opposite subunit partially occluding the active site and a C-terminal widget consisting of random coil and a short α -helix.

The most unusual and functionally significant aspect of the structure is the fact that each active site harbors two molecules of GSH bound in an antiparallel arrangement with the two sulfur atoms adjacent to one another at a distance of 3.4 Å (Figure 3). Together, the two GSH molecules resemble a molecule of GSSG except that an omit map of the electron density in the active site clearly reveals that there is little if no density to correspond with a disulfide bond (Figure 3). The refined distance of 3.4 Å between the two sulfur atoms is reasonable for a hydrogen bond between a thiolate anion and a thiol and much longer than that of a disulfide bond.

The details of the binding of the two GSH molecules to YghU are illustrated in Figure 4. One molecule of GSH (GSH1) is bound in a canonical fashion with the sulfhydryl

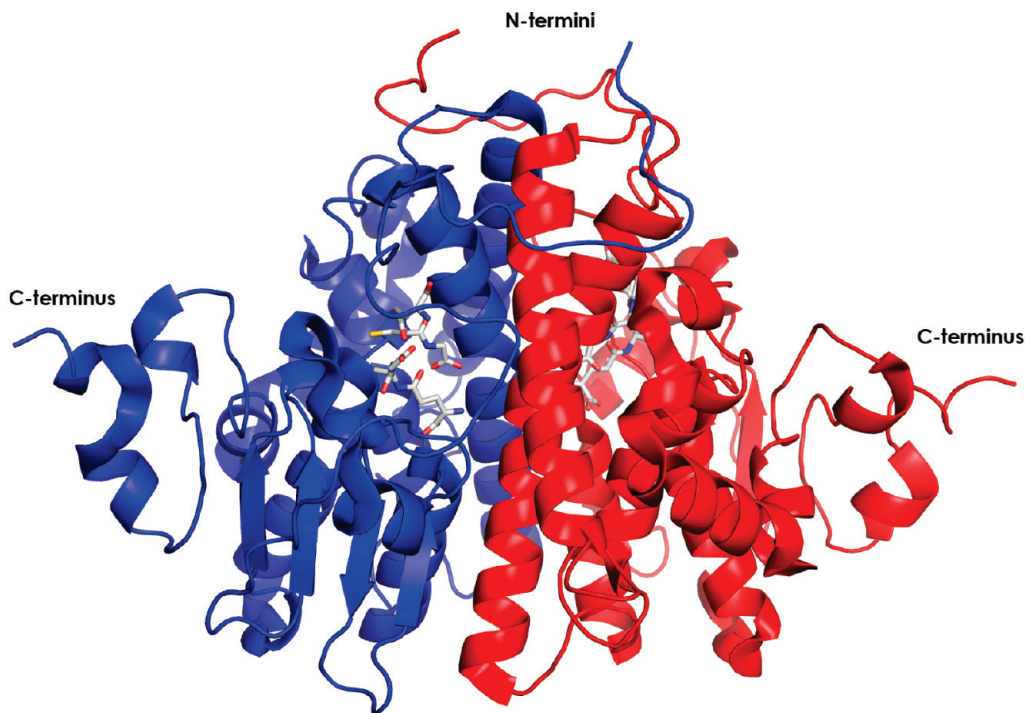


FIGURE 2: Ribbon diagram of the structure of YghU as determined at a resolution of 1.50 Å. The two subunits are colored blue and red. The N-termini of each polypeptide are shown at the top. The C-termini of each subunit are shown at the left and right. The four molecules of GSH are illustrated as stick diagrams in each subunit.

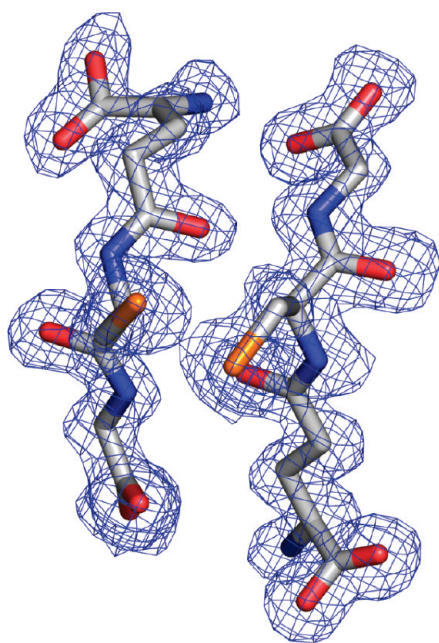


FIGURE 3: Omit map of the electron density for the two molecules of GSH observed in the active site of YghU. The map, contoured at 2.5σ , was calculated with coefficients of the form $F_o - F_c$ in which the observed and calculated structure factor amplitudes were calculated from the model lacking the coordinates of the two molecules of GSH. The final model of the two molecules is shown in stick representation. The two sulfur atoms in the middle are colored orange.

group located at the end of α -helix 1 within hydrogen-bonding distance of the hydroxyl group of T54. GSH1 has seven potential hydrogen-bond contacts with the protein, including two with the sulfhydryl group. The second molecule (GSH2) has only four direct hydrogen-bonding contacts with the protein mediated by R178 located on the opposite subunit and N26 that is located in

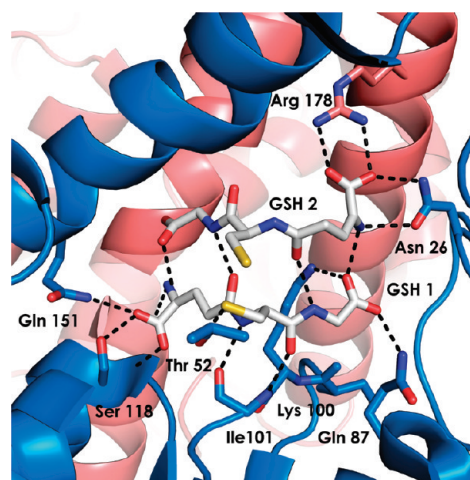


FIGURE 4: Details of the potential hydrogen-bonding interactions of the two GSH molecules in the active site of YghU. The primary subunit is colored blue and the opposing subunit red. The two GSH molecules are shown in stick representation. The sulfur atoms are colored yellow.

the N-terminal tail of the protein. In their antiparallel arrangement, the two GSH molecules share four mutual hydrogen-bonding interactions, including one between the two sulfur atoms. The average B factor for atoms in GSH1 is 9.9 \AA^2 , whereas it is 14.0 \AA^2 for GSH2. This observation is consistent with the fact but does not prove that GSH1 is the more tightly bound molecule observed in the titration experiments.

The Structure Reveals Function. The juxtaposition of the two molecules of GSH in the active site of the crystal structure of the enzyme suggests that YghU might facilitate redox reactions. Some GSH transferases have long been known to catalyze organic hydroperoxidase reactions (26). YghU, with its two aligned molecules of GSH, would appear to be uniquely set up

Table 2: Kinetic Constants for Reactions Catalyzed by YghU with Various Organic Hydroperoxides at 25 °C

substrate	k_{cat} (s^{-1})	$K_{\text{M}}^{\text{ROOH}}$ (μM)	$k_{\text{cat}}/K_{\text{M}}^{\text{ROOH}}$ ($\text{M}^{-1} \text{s}^{-1}$)
cumene-OOH	0.050 ± 0.001	16 ± 2	3500 ± 400
13(S)-linoleic-OOH	0.19 ± 0.02	130 ± 30	1500 ± 400
15(S)-HpETE	0.096 ± 0.004	28 ± 4	3400 ± 1500

for the efficient reduction of peroxides. The enzyme does not reduce H_2O_2 or *tert*-butyl hydroperoxide at appreciable rates but does have modest activity with some other organic hydroperoxides, as summarized in Table 2. Although the turnover numbers are low, the values of $k_{\text{cat}}/K_{\text{M}}^{\text{ROOH}}$ suggest that these types of molecules are potential natural substrates for YghU. However, it is important to point out that if this is true, the identities of specific hydroperoxide substrates remain to be discovered.

Another obvious function of YghU is that of a disulfide-bond oxidoreductase, like its structural homologue, YfcG (9). In this regard, YghU was found to have good catalytic activity toward 2-hydroxyethyl disulfide with a k_{cat} of $74 \pm 6 \text{ s}^{-1}$ and a $k_{\text{cat}}/K_{\text{M}}^{\text{GSH}}$ of $(6.4 \pm 1.3) \times 10^4 \text{ M}^{-1} \text{ s}^{-1}$. These kinetic constants are very close to those recently determined for YfcG [$k_{\text{cat}} = 29 \pm 2 \text{ s}^{-1}$, and $k_{\text{cat}}/K_{\text{M}}^{\text{GSH}} = (1.8 \pm 0.3) \times 10^4 \text{ M}^{-1} \text{ s}^{-1}$]³ and are on par with those previously measured for various thioredoxins and glutaredoxins (27). YghU appears to be a reasonably efficient disulfide-bond reductase by virtue of its ability to bind two molecules of GSH in the proximity of the active site.

DISCUSSION

A New Class of GSH Transferases. YghU has structural and functional properties that are remarkably similar to those of YfcG (9). Both enzymes have some activity toward organic hydroperoxides, with YghU being superior in that particular regard. More interesting is their robust disulfide-bond reductase activity toward 2-hydroxyethyl disulfide. Both proteins are as good in this assay as other efficient disulfide-bond reductases such as glutaredoxin and thioredoxin (27). The sequence similarity of the two proteins, illustrated in Figure S1 (Supporting Information), makes a compelling argument that the proteins are related in both structure and function. The major differences are the N-terminal and C-terminal extensions observed in YghU but not in YfcG. The crystal structure of YghU indicates that N26 of the N-terminal extension interacts directly with GSH2. Whether this is an artifact of crystal packing or of some biological significance is not yet known.

The cores of the two proteins are quite similar, especially in the thioredoxin domain. Of particular note is the apparent hydrogen-bonding interaction between the hydroxyl group of a threonine residue located at the end of the first α -helix of the thioredoxin domain and the sulfur of GSH1. Most GSH transferases have an electrophilic side chain located at the N-terminal end of α -helix 1 that assists in stabilizing the glutathione thiolate. These residues are typically tyrosine, serine, or cysteine and serve as one of the structural delineations between the various classes of GSH transferases (28). YghU and YfcG are the first structurally

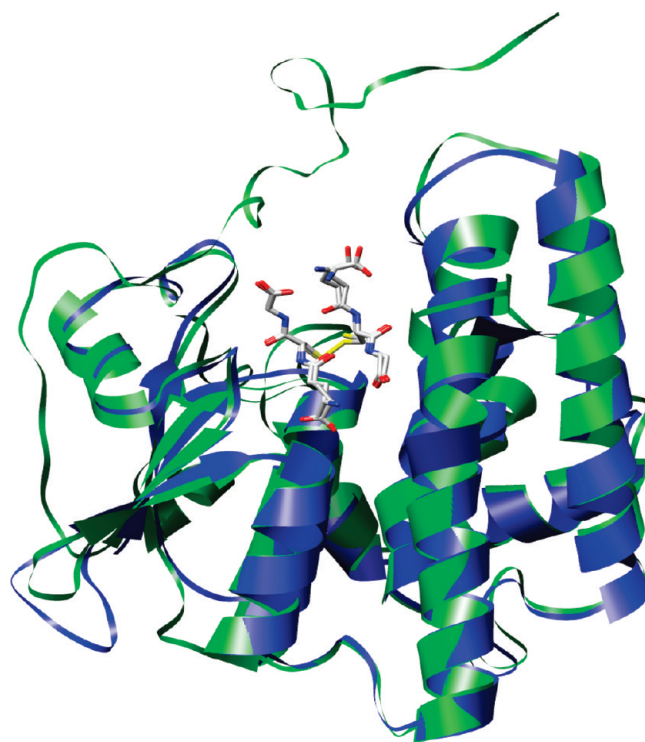


FIGURE 5: Overlay of the subunit structures of YfcG (blue) and YghU (green). The two GSH molecules associated with YghU and the GSSG molecule bound to YfcG are shown in stick representation. The long N-terminal extension of YghU can be seen at the top.

confirmed examples of GSH transferases that utilize a threonine hydroxyl group in this capacity.

An even more compelling argument concerning the relationship of YfcG and YghU can be made from an overlay of their three-dimensional structures as illustrated in Figure 5. The close superposition of each polypeptide chain is not too surprising given their sequence similarity. More striking is the very close superposition of the two GSH molecules (in YghU) and the molecule of GSSG in YfcG. The concurrence of the threonine residues that interact with the sulfur of GSH (or GSSG) and the arginine residues (Figures 4 and 5 and Figure S1 of the Supporting Information) from the opposite subunit that interact with the second molecule of GSH or second half of GSSG in the case of YfcG (9) are a structural signature of a new class of GSH transferase-like proteins that appear to principally function as disulfide-bond oxidoreductases. In very recent preliminary experiments associated with the Enzyme Function Initiative, the high-throughput screening of the activities of more than 50 microbial proteins from the GST superfamily detected another member of this family from *Pseudomonas fluorescens* (Figure S1 of the Supporting Information). This protein has the sequence signature of this new class of GSH transferases and a robust disulfide-bond reductase activity, as well.

Nu-Class GSH Transferases. The evidence described above suggests that YfcG and YghU from *E. coli* are the charter members of a new class of GSH transferases that have unique structural and functional properties, which allow them to bind and utilize GSSG or a GSH pair in a fashion that promotes disulfide-bond oxidoreductase reactions. It is important to point out that a robust disulfide-bond reductase activity is not a common one for GSH transferases and appears to be confined to those enzymes that can accommodate two GSH molecules in their active sites. For example, of the other GSH transferases

³The originally reported steady-state kinetic constants for YfcG, which were in error because of a mistake in the calculation of k_{cat} , have now been corrected (33).

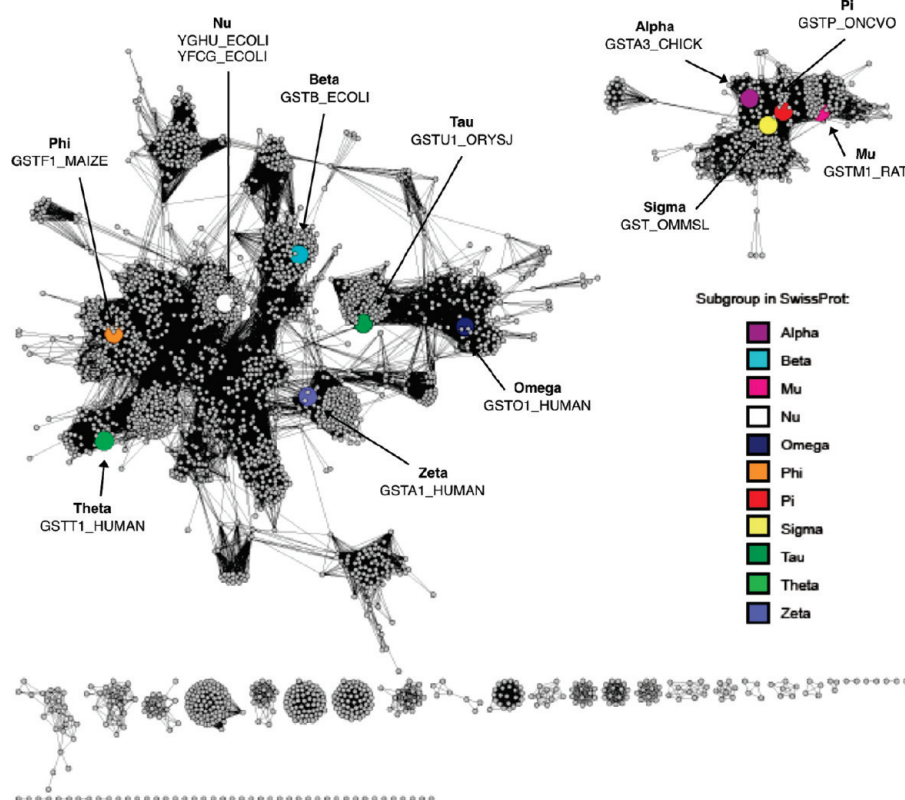


FIGURE 6: YfcG and YghU form a nu class of GSH transferases. The overall sequence similarity network contains 2851 sequences and 97144 edges. Edges represent BLAST E values of 10^{-18} or more stringent. Large nodes are colored by the classification of the amino acid sequence in SWISS-PROT and indicate a representative member of each subgroup as follows: alpha, GSTA3_CHICK (UniProt accession number P26697); beta, GSTB_ECOLI (P0ACA7); mu, GSTM1_RAT (P04905); nu, YFCG_ECOLI (P77526) and YGHU_ECOLI (Q46845); omega, GSTO_HUMAN (P78417); phi, GSTF1_MAIZE (P12653); pi, GSTP_ONCVO (P46427); sigma, GST_OMMSL (P46088); tau, GSTU1_ORYSJ (Q10CE7); theta, GSTT1_HUMAN (P30711); zeta, GSTZ1_HUMAN (O43708).

from *E. coli*, only two, EGST (29) and YqjG (M. C. Branch and R. N. Armstrong, unpublished results), have very low and modest disulfide-bond reductase activities, respectively. It is important to note that both of the proteins have an active-site cysteine residue in the proximity of the thiol of bound GSH.

In the tradition of naming various subfamilies of GSH transferases with a Greek letter such as alpha, mu, pi, sigma, phi, beta, omega, zeta, theta, tau, zeta, and kappa (28, 30–32), we suggest that this particular subfamily be designated as nu. Although there is no published standard for naming bacterial GSH transferases, we further propose that YfcG be designated GST N1-1 and that YghU be designated GST N2-2.

Viewing the nu-class enzymes in the wider context, we find the universe of GSH transferase folds clearly suggests that the two *E. coli* proteins (YghU and YfcG) and a number of others from different organisms cluster close together as shown in Figure 6. This cluster is located in the center of a large group of GSH transferases from bacteria, plants, and animals, suggesting it may represent a widely distributed subfamily.

Conclusions. The YghU and YfcG proteins encoded in the genome of *E. coli* represent a previously unrecognized class of GSH transferases that have unique structural and catalytic properties. The nu-class GSH transferases have a distinct active site and the ability to bind GSSG with high affinity or two molecules of GSH simultaneously. That property confers on these proteins disulfide-bond oxidoreductase or organic hydroperoxidase activity. YghU and YfcG have very significant chemical and structural differences, including their preferred oxidation states and the N- and C-terminal extensions of YghU

that might be keys to the differentiation of their biological functions. Preliminary results suggest that similar proteins exist in other Gram-negative microorganisms.

ACKNOWLEDGMENT

We thank the Enzyme Function Initiative (supported by National Institutes of Health Grant U54 GM093342-01, J. A. Gerlt, Principle Investigator) and in particular Prof. Patsy Babbitt and Dr. Shoshana Brown (University of California, San Francisco) for help with the bioinformatics aspects of this paper. Use of the Advanced Photon Source was supported by the U.S. Department of Energy, Office of Science, Office of Basic Energy Sciences, under Contract W-31-109-Eng-38.

SUPPORTING INFORMATION AVAILABLE

Sequence alignments of YfcF, YfcG, and a related protein with robust disulfide-bond reductase activity (Figure S1). This material is available free of charge via the Internet at <http://pubs.acs.org>.

REFERENCES

1. Rife, C. L., Parsons, J. F., Xiao, G., Gilliland, G. L., and Armstrong, R. N. (2003) Conserved Structural Elements in Glutathione Transferase Homologues Encoded in the Genome of *Escherichia coli*. *Proteins: Struct., Funct., Genet.* 53, 777–782.
2. Koonin, E. V., Mushegian, A. R., Tatusov, R. L., Altschul, S. F., Bryant, S. H., Bork, P., and Valencia, A. (1994) Eukaryotic translation elongation factor 1 γ contains a glutathione transferase domain: Study of a diverse, ancient protein superfamily using motif search and structural modeling. *Protein Sci.* 3, 2045–2054.

3. Bai, M., Zhou, J. M., and Perett, S. (2003) The yeast prion protein Ure2 shows glutathione peroxidase activity in both native and fibrillar forms. *J. Biol. Chem.* 279, 50025–50030.
4. Dulhunty, A., Gage, P., Curtis, S., Chelvanayagam, G., and Board, P. (2001) The Glutathione Transferase Structural Family Includes a Nuclear Chloride Channel and a Ryanodine Receptor Calcium release Channel Modulator. *J. Biol. Chem.* 276, 3319–3323.
5. Harrop, S. J., DeMaere, M. Z., Fairlie, W. D., Reztsova, T., Valenzuela, S. M., Mazzanti, M., Tonini, R., Qui, M. R., Jankova, L., Warton, K., Bauskin, A. R., Wu, W. M., Pankhurst, S., Campbell, T. J., Breit, S. N., and Curmi, P. M. G. (2001) Crystal structure of the soluble form of the intracellular chloride ion channel CLIC1 (NC27) at 1.4 Å resolution. *J. Biol. Chem.* 276, 44993–45000.
6. Williams, M. D., Ouyang, T. X., and Flickinger, M. C. (1994) Starvation induced expression of SspA and SspB: The effects of a null mutation in sspA on *Escherichia coli* protein synthesis and survival during growth and prolonged starvation. *Mol. Microbiol.* 11, 1029–1060.
7. Hansen, A. M., Qui, Y., Yeh, N., Blattner, F. R., Durfee, T., and Jin, D. J. (2005) SspA is required for acid resistance in stationary phase by down regulation of H-NS in *Escherichia coli*. *Mol. Microbiol.* 56, 719–734.
8. Hansen, A. M., Gu, Y., Li, M., Andrykovitch, M., Waugh, D. S., Jin, D. J., and Ji, X. (2005) Structural basis for the function of stringent starvation protein A as a transcription factor. *J. Biol. Chem.* 280, 17380–17391.
9. Wadington, M. C., Ladner, J. E., Stourman, N. V., Harp, J. M., and Armstrong, R. N. (2009) Analysis of the Structure and Function of YfcG from *Escherichia coli* Reveals an Efficient and Unique Disulfide Bond Reductase. *Biochemistry* 48, 6559–6561.
10. Tabor, H., and Tabor, C. W. (1975) Isolation, Characterization and Turnover of Glutathionylspermidine from *Escherichia coli*. *J. Biol. Chem.* 250, 2649–2654.
11. Smith, K., Borges, A., Ariyanayagam, M. R., and Fairlamb, A. H. (1995) Glutathionylspermidine metabolism in *Escherichia coli*. *Biochem. J.* 312, 465–469.
12. Stourman, N. V., Wadington, M. C., Schaab, M. R., Atkinson, H. J., Babbitt, P. C., and Armstrong, R. N. (2008) Functional genomics in *Escherichia coli*: Experimental approaches for the assignment of enzyme function. In Proceedings of the 3rd International Beilstein Workshop on Experimental Standard Conditions of Enzyme Characterizations (Hicks, M. G., and Kettner, C., Eds.) pp 1–12, Beilstein Institut, Frankfurt am Main, Germany.
13. Bollinger, J. M., Jr., Kwon, D. S., Huisman, G. W., and Walsh, C. T. (1995) Glutathionylspermidine Metabolism in *Escherichia coli*. *J. Biol. Chem.* 270, 14031–14041.
14. Vlamis-Gardikas, A., Åslund, F., Spyrou, G., Bergman, T., and Holmgren, A. (1997) Cloning, Overexpression and Characterization of Glutaredoxin 2, an Atypical Glutaredoxin from *Escherichia coli*. *J. Biol. Chem.* 272, 11236–11243.
15. Iacazio, G., Langrand, G., Baratti, J., Buono, G., and Triantaphylides, C. (1990) Preparative, enzymic synthesis of linoleic acid (13S)-hydroperoxide using soybean lipoxygenase-1. *J. Org. Chem.* 55, 1690–1691.
16. Flohé, L., and Günzler, W. A. (1984) Assays of Glutathione Peroxidase. *Methods Enzymol.* 105, 115–120.
17. Jakobsson, P., Mancini, J., Riendeau, D., and Ford-Hutchinson, A. (1997) Identification and Characterization of a Novel Microsomal Enzyme with Glutathione-dependent Transferase and Peroxidase Activities. *J. Biol. Chem.* 272, 22934–22939.
18. Lakowicz, J. R. (1999) Principles of Fluorescence Spectroscopy, 2nd ed., pp 53–55, Kluwer Academic/Plenum Publishers, New York.
19. Otwinowski, Z., and Minor, W. (1997) Processing of X-ray diffraction data collected in oscillation mode. *Methods Enzymol.* 276, 307–326.
20. Schneider, T. R., and Sheldrick, G. M. (2002) Substructure solution with SHELXD. *Acta Crystallogr. D* 58, 1772–1779.
21. Schneider, T. R., and Sheldrick, G. M. (2002) Macromolecular phasing with SHELXE. *Z. Kristallogr.* 217, 644–650.
22. Pape, T., and Schneider, T. R. (2004) HKL2MAP: A graphical user interface for phasing with SHELX programs. *J. Appl. Crystallogr.* 37, 843–844.
23. Morris, R. J., Perrakis, A., and Lamzin, V. S. (2003) ARP/wARP and automatic interpretation of protein electron density maps. *Methods Enzymol.* 374, 229–244.
24. McRee, D. E. (1999) XtalView/Xfit: A versatile program for manipulating atomic coordinates and electron density. *J. Struct. Biol.* 125, 156–165.
25. Murshudov, D. N., Vagin, A. A., and Dodson, E. J. (1997) Refinement of Macromolecular Structures by the Maximum-Likelihood Method. *Acta Crystallogr. D* 53, 140–255.
26. Prohaska, J. R., and Ganther, J. E. (1977) Glutathione Peroxidase Activity of Glutathione S-Transferases Purified from Rat Liver. *Biochem. Biophys. Res. Commun.* 76, 437–445.
27. Berndt, C., Lillig, C. H., and Holmgren, A. (2008) Thioredoxins and Glutaredoxins as Facilitors of Protein Folding. *Biochim. Biophys. Acta* 1783, 641–650.
28. Armstrong, R. N. (1997) Structure, Catalytic Mechanism and Evolution of the Glutathione Transferases. *Chem. Res. Toxicol.* 10, 1–18.
29. Wang, X. Y., Zhang, Z. R., and Perrett, S. (2009) Characterization of the activity and folding of the glutathione transferase from *Escherichia coli* and the roles of residues Cys(10) and His(106). *Biochem. J.* 417, 55–64.
30. Mannervik, B., and Danielson, U. H. (1988) Glutathione Transferases: Structure and Catalytic Activity. *CRC Crit. Rev. Biochem.* 23, 283–337.
31. Mannervik, B., Awasthi, Y. C., Board, P. G., Hayes, J. D., Di Ilio, C., Ketterer, B., Listowsky, I., Morgenstern, R., Muramatsu, M., and Pearson, W. R. (1992) Nomenclature for Human Glutathione Transferases. *Biochem. J.* 282, 305–306.
32. Atkinson, H. J., and Babbitt, P. C. (2009) Glutathione Transferases Are Structural and Functional Outliers in the Thioredoxin Fold. *Biochemistry* 48, 11108–11116.
33. Wadington, M. C., Ladner, J. E., Stourman, N. V., Harp, J. M., and Armstrong, R. N. (2010) Correction to Analysis of the Structure and Function of YfcG from *Escherichia coli* Reveals an Efficient and Unique Disulfide Bond Reductase. *Biochemistry* 49, 10765.